arXiv:2104.05570v3 [cs.CV] 12 Oct 2021

Learning from Subjective Ratings Using Auto-Decoded Deep Latent Embeddings

Bowen Li[1], Xinping Ren[2], Ke Yan[1], Le Lu[1], Lingyun Huang[4], Guotong Xie[4], Jing Xiao[4], Dar-In Tai[3], and Adam P. Harrison[1]

[1] PAII Inc., Bethesda, MD 20817, USA
[2] Ruijin Hospital, Shanghai, China
[3] Chang Gung Memorial Hospital, Linkou, Taiwan, ROC
[4] PingAn Technology, Shenzhen, China

Abstract. Depending on the application, radiological diagnoses can be associated with high inter- and intra-rater variabilities. Most computer-aided diagnosis (CAD) solutions treat such data as incontrovertible, exposing learning algorithms to considerable and possibly contradictory label noise and biases. Thus, managing subjectivity in labels is a fundamental problem in medical imaging analysis. To address this challenge, we introduce auto-decoded deep latent embeddings (ADDLE), which explicitly models the tendencies of each rater using an auto-decoder framework. After a simple linear transformation, the latent variables can be injected into any backbone at any and multiple points, allowing the model to account for rater-specific effects on the diagnosis. Importantly, ADDLE does not expect multiple raters per image in training, meaning it can readily learn from data mined from hospital archives. Moreover, the complexity of training ADDLE does not increase as more raters are added. During inference each rater can be simulated and a "mean" or "greedy" virtual rating can be produced. We test ADDLE on the problem of liver steatosis diagnosis from 2D ultrasound (US) by collecting 36 602 studies along with clinical US diagnoses originating from 65 different raters. We evaluated diagnostic performance using a separate dataset with gold-standard *biopsy* diagnoses. ADDLE can improve the partial areas under the curve (AUCs) for diagnosing severe steatosis by 10.5% over standard classifiers while outperforming other annotator-noise approaches, including those requiring 65 times the parameters.

Keywords: Subjective Labels · Latent Embedding · Liver Steatosis · Ultrasound.

1 Introduction

Deep learning has been widely applied to computer-aided diagnosis (CAD) tasks [18,3]. In order to train effective deep neural networks, large-scale labeled datasets are needed [8,22]. Yet, the labels within large-scale data, such as those found within hospital picture archiving and communication systems (PACSs), are typically image-based diagnoses, which are not always considered "ground-truth" [22]. Take for instance liver steatosis (fatty liver) diagnosis. Liver biopsy is considered the gold standard diagnosis for liver steatosis, but the risks and costs associated with such procedures hinder the collection of large-scale data. On the other hand, ultrasound (US) is the most common tool for

assessing liver steatosis [12] and image/US-diagnosis pairs can be readily mined from PACSs. Unfortunately, US diagnoses are considered subjective and suffer from considerable inter- and intra-rater variability [12]. Thus, CAD solutions are faced with the quandary of needing to produce quantitative diagnostic scores when only subjectively labelled training data is available.

The problem of annotator noise has historically been addressed using expectation-maximization (EM) approaches [5,21,14], which typically attempt to estimate true labels and a conditional model that explains rater labels. However, apart from Khetan *et al.* [14], these require multiple ratings per sample, which is not a realistic requirement for large-scale data, especially for clinical PACS data. Another approach for annotator noise is multi-rater consensus modeling (MRCM) [25], which relies on a consensus loss that is only meaningful in a multiple rating per sample scenario. STAPLE is another popular EM approach that is used to impute ground truth from noisy labels [20], but it has the same multiple-rater requirements. In our problem setting and most clinical scenarios, there is only one rater annotating one image. Our solution is able to work with multi-rater data, but multi-rater algorithms cannot work with our data. In terms of methods that do not assume multi-ratings per training sample, Tanno *et al.* proposed an approach to estimate annotator confusion matrices that avoids the complexity of EM [19], but they assume that any annotator noise is dependent only on the true label and independent of the image itself, which will likely be violated. Another common limitation of the above approaches is that they are only applicable for categorical classification. More akin to our approach, some recent investigations have explicitly modelled each individual rater. For instance Chou *et al.* train separate models for each individual or group of raters [4], but this is very computationally expensive. Guan *et al.* train a separate classification head for each rater [9], but this is limited in modelling capability and their final solution requires a weighted average that again relies on multiple raters per sample, which are needed to calculate weights.

To fill these gaps, we introduce auto-decoded deep latent embeddings (ADDLE). In contrast to these above approaches, ADDLE models individual raters using a rich and expressive latent embedding that is probabilistically motivated. After a linear transformation to match dimensions, the encodings in rater-specific latent vectors can be added to convolutional or global features. The latent vector values, along with shared backbone weights, that best predict each rater's labels are then learned. ADDLE avoids the complexity of EM approaches and can be readily trained using typical gradient descent procedures. Additionally, although it admits multiple raters per sample, ADDLE naturally works with single ratings per sample, addressing the most critical use-case within CAD. Moreover, ADDLE correctly models subjective ratings as conditional on both the image itself and the true label. Finally, ADDLE imposes no restrictions on what loss can be used and can be readily applied to any medical imaging task, including classification, detection, or segmentation.

We validate ADDLE on the task of liver steatosis diagnosis using conventional liver US images. Liver steatosis affects $20-30\%$ of the global population and is associated with serious risk factors, such as liver fibrosis and hepatocellular carcinoma [24]. We trained ADDLE on a large-scale multi-scanner and multi-etiology PACS-mined dataset of image/US diagnosis pairs (3 790 patients, 312 848 images, and 36 602 studies) that

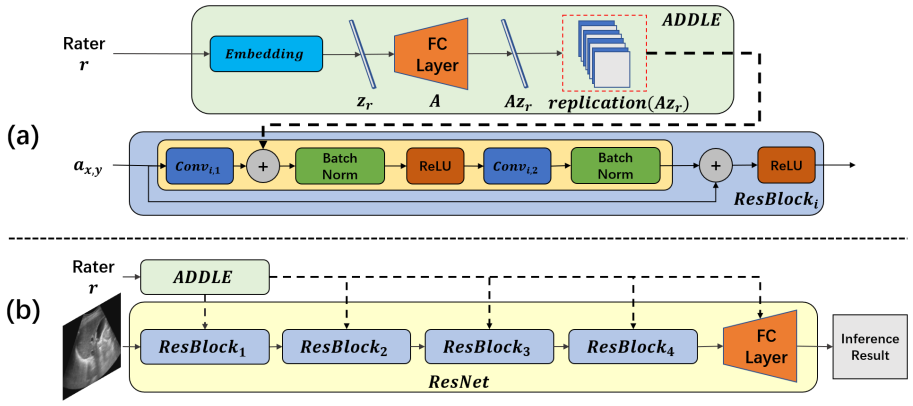


Fig. 1. Algorithmic workflow of ADDLE. (a): ADDLE and its integration into a ResBlock. (b): Potential injection points of ADDLE into a ResNet. ADDLE can also be used with any other classifcation, detection, or segmentation backbone.

were labelled by 65 different clinicians during clinical care. Apart from our methodological contributions, this alone represents a significant contribution in its own right. Deep learning has previously been applied to liver US, such as for diagnosing steatosis [2,1,10,17], diagnosing fibrosis [15], and detecting lesions [23]. For liver steatosis, datasets are small, with less than 200 patients and less than 1000 images [2,1,10,17] with only single scanners and etiologies, so method generalizability is under-tested.

In terms of methodological contributions, we show that ADDLE can learn from and model subjective US diagnoses. We evaluated ADDLE on a separate dataset of 148 patients with biopsy-proven diagnoses and show that the "mean" and "greedy" ADDLE virtual raters can outperform both standard classification baselines and also leading annotator noise approaches [9,4] in discriminating between healthy, mild, moderate, and severe steatosis. These results demonstrate that ADDLE provides a flexible, straightforward, and effective approach to manage subjectivity in medical imaging labels.

2 Methods

Fig. 1 depicts the workings of ADDLE. In short, we assume we are given a dataset of images, noisy/subjective labels, and rater indices $\mathcal{X} = \{\mathbf{x}_i, y_i, r\}_{i=1}^{N}$ where $r = 1, \ldots R$ indexes which rater generated the label. Here for simplicity we assume a single rater per image and image-level labels, but ADDLE can easily admit multiple raters and other label types. We describe the training and inference process below.

Training Park *et al.* [16] introduced an auto-decoder-based method, which learns the latent space of shapes for shape representation. ADDLE uses a similar approach to create rater-specific latent embeddings. We associate a set of latent codes, $\mathcal{Z} = \{\mathbf{z}_r\}_{r=1}^{R}$, to the raters. In practical terms, each $\mathbf{z}_r$ is a simple vector. We model the mapping from

images and latent embeddings to a subjective rating using a deep network, $f_\theta(\mathbf{x}_i, \mathbf{z}_r)$, that accepts both the image and the corresponding latent code as input. The deep network can be any popular or well-known network that would normally accept the $\mathbf{x}_i$ input. We can inject the latent codes to any convolutational or global feature map along the network's forward propagation path via simple addition. In this way, the shared neural net weights encode common features that can be influenced by the latent embeddings to model any rater-specific tendencies. To retain any pretrained weights, we only inject the latent codes as part of an existing convolutional or fully-connected layer. For instance, if the latent code dimensionality is M and we wish to inject the latent codes in conjunction with a convolution with C outputs operating on a feature map, $\mathbf{a}_{x,y}$, we simply apply a linear transformation and replication operation:

$$\tilde{\mathbf{a}}_{x,y} = \mathrm{conv}(\mathbf{a}_{x,y}) + \mathrm{rep}(\mathbf{A}\mathbf{z}_r), \tag{1}$$

where $\tilde{\mathbf{a}}_{x,y}$ is the output feature map, $\mathrm{conv}(.)$ is the convolutional operator, $\mathbf{A}$ is an $C \times M$ matrix, and $\mathrm{rep}(.)$ replicates a vector across the convolutional spatial dimensions. Due to the linearity of convolution, (1) operates as if a large convolution was applied to a concatenated feature representation of $\mathbf{a}_{x,y}$ and $\mathbf{z}_r$. Importantly, any original pretrained weights in $\mathrm{conv}(.)$ can be kept. If injected to a global feature, the $\mathrm{rep}(.)$ operator can be forgone. Finally, if beneficial ADDLE allows latent codes to be injected at multiple points.

To learn the latent codes, we formulate a posterior composed of a product between a prior distribution and the likelihood of the observed labels:

$$p_\theta(\mathcal{Z}|\mathcal{X}) = \prod_r p(\mathbf{z}_r) \prod_{\{\mathbf{x}_i, y_i\} \in \mathcal{X}_r} p_\theta(y_i|\mathbf{x}_i, \mathbf{z}_r), \tag{2}$$

where $\mathcal{X}_r$ selects all samples labelled by the rth rater and θ parameterizes the likelihood. We assume that the prior, $p(\mathbf{z}_r)$, follows an isotropic zero-mean Gaussian distribution with a covariance of $\sigma^2\mathbf{I}$ (which is also how we initialize the latent embeddings). Given any loss, $\mathcal{L}(.,.)$, the likelihood can be expressed using the deep neural network described above:

$$p_\theta(y_i|\mathbf{x}_i, \mathbf{z}_r) = \exp(-\mathcal{L}(f_\theta(\mathbf{x}_i, \mathbf{z}_r), y_i)). \tag{3}$$

Loss functions are not constrained to be classification-based—indeed our own experiments employ an ordinal regression formulation. During training, (2) is maximized by minimizing the following sum with respect to the rater codes, $\mathcal{Z}$, and the shared network parameters, θ:

$$\underset{\theta,\, \mathcal{Z}}{\arg\min} \sum_{\{\mathbf{x}_i, y_i, r\} \in \mathcal{X}} (\mathcal{L}(f_\theta(\mathbf{x}_i, \mathbf{z}_r), y_i)) + \sum_{r=1}^{R} \left(\frac{1}{\sigma^2} ||\mathbf{z}_r||_2^2 \right), \tag{4}$$

which can be trained using gradient descent. The auto-decoding nature of ADDLE comes from the fact there is no encoding function for the latent embeddings. Instead the latent embedding values are learned solely based on the loss and prior formulation in (4). One downside of (4) is that if there are unbalanced numbers of samples labeled

by the raters, then poorly represented raters may not be well optimized. To deal with this, after a solution to (4) is found the shared weights can be frozen and each rater's latent embedding can be individually fine-tuned:

$$\arg\min_{\mathbf{z}_r} \sum_{\{\mathbf{x}_i, y_i\} \in \mathcal{X}_r} (\mathcal{L}(f_\theta(\mathbf{x}_i, \mathbf{z}_r), y_i)) + \frac{1}{\sigma^2} ||\mathbf{z}_r||_2^2, \tag{5}$$

where only the rater's samples, $\mathcal{X}_r$, are selected. Optimizing (5) is quick, since only each rater's latent vector needs to be fine-tuned, which are small in dimension.

Inference After training, ADDLE should model how each rater would label a new image. But, emulating rater subjectivity alone is not necessarily useful in inference. Because ADDLE can provide simulated predictions for each rater, if there is *a priori* information on which raters are more experienced or trustworthy, ADDLE could simply simulate those ones. More generally, this is not available. One option is to greedily choose the "best" raters to average using a validation set with gold-standard diagnoses:

$$\bar{y} = \frac{1}{R} \sum_{r \in \mathcal{R}_{\text{greedy}}} f_\theta(\mathbf{x}_i, \mathbf{z}_r), \tag{6}$$

where $\mathcal{R}_{\text{greedy}}$ is a set of raters that are greedily chosen until validation performance tops out. When such validation sets are not available ADDLE can output a mean or majority rating:

$$\bar{y} = \frac{1}{R} \sum_{r=1}^{R} f_\theta(\mathbf{x}_i, \mathbf{z}_r). \tag{7}$$

3 Experiments

Datasets We test ADDLE on the problem of liver steatosis diagnosis from US. Because US is the most common modality for clinically assessing liver steatosis, it is possible to collect large-scale datasets for algorithmic training. To this end, we collected a big-data (**BD**) cohort consisting of 3 790 patients, 312 848 US images, and 36 602 US studies from the PACS of *Anonymized*. Through the course of clinical care, each study was given a four-class ordinal assessment of either healthy, mild, moderate, or severe steatosis from one of 65 clinicians. We used 3 405 patients for training and left the rest as a stopping criteria validation set. We evaluated whether the ADDLE greedy and mean raters of (6) and (7), respectively, can provide a better quantitative score to differentiate more objective histopathology-derived steatosis severities. To do this we collected a separate histopathology (**HP**) dataset of 218 patients and US studies, all with accompanying biopsy-proven diagnoses within 3 months of the scan date. Histopathological diagnoses follow the same ordinal configuration from healthy to severe steatosis as the US ones. We used 70 of the patients for validation (**HP**-V), but only for model selection and greedy rater selection, and *not* as a validation set for stopping criteria. This left 148 patients as a test set (**HP**-T), with 25, 35, 36, and 52 diagnosed with healthy, mild,

moderate, and severe steatosis, respectively . Patients with hepatitis B, hepatitis C, and non-alcoholic fatty liver disease are all represented in **BD** and **HP** studies originated from three different scanners with images corresponding to the six different viewpoints described by Li *et al.* [15].

Setup The well-known binary decomposition loss of Frank and Hall for ordinal regression [6,7] was used for training on the ordered US severity labels. We used a ResNet-18 [11] backbone, which proved the most optimal, choosing a latent embedding dimensionality of 10, injecting the latent codes at the beginning of the second residual block, and using a σ^2 value of 1.0. An analysis of hyper-parameter sensitivity, found in the supplementary, indicates that performance was not sensitive to the choice of σ^2 and was stable across most injection points and latent code sizes. Once trained, a simple summation of the Frank and Hall outputs can produce a single score [7]. In training we treat each US image in a study as an independent sample, but in inference we take the mean score across all images in a study to produce a study-wise score. Analysis on **HP**-V indicated that the top-two raters should be used for the greedy ADDLE variant of (6).

As baselines, we compare ADDLE to both a standard ResNet-18 network trained on **BD**'s US labels (denoted ResNet-18-**BD**) and a ResNet-18 trained only on the small-scale **HP**-T dataset using five-fold cross validation (denoted ResNet-18-**HP**). Comparisons with these baselines respectively reveal the impact of modelling rater tendencies and the importance of using large-scale data for training, even should it be subjectively labelled. We also compared against annotator noise methods that permit ordinal regression. The first comparison uses Chou *et al.*'s JLSL approach of training a separate model for each rater [4]. Note, Chou *et al.* also used additional components, but these rely on multiple raters per sample or the availability of gold-standard labels during training (which we do not assume), so we only evaluate the idea of a single model per rater. We also evaluate Guan *et al.*'s multi-head approach of using a separate classification layer for each rater [9], but forego their weighting process that also assumes multiple raters per sample. In short, JLSL [4] trains a separate model for each rater and multi-head [9] trains a separate classification head. Because we test on the same backbone, their implementation details are identical to ADDLE's apart from the above critical differences. For fairness, we finetune multi-head using an analogous version of (5). Like ADDLE, for each we evaluate their "mean" and "greedy" rater performance.

Evaluation Protocols Because the problem is to discriminate between four ordered histopathological grades, standard binary receiver operating characteristic (ROC) analysis cannot be performed. Following standard practice, we use ROC analysis on three different and ordered binary *cutoffs*, specifically $>=$ mild, $>=$ moderate, or $=$ severe levels of steatosis. Associated AUC summary statistics for these cutoffs are denoted AUC_0, AUC_1, and AUC_2, respectively. Like was done by Li *et al.* for liver fibrosis [15], we primarily focus on partial ROC curves and AUCs only within the range of false positive rates that are $<= 30\%$. The reasoning being that lower specificities are not clinically useful operating points to investigate. Partial AUCs are normalized to be within a range of 0 to 1. Additionally, we also report Jonckheere-Terpstra (JT) index

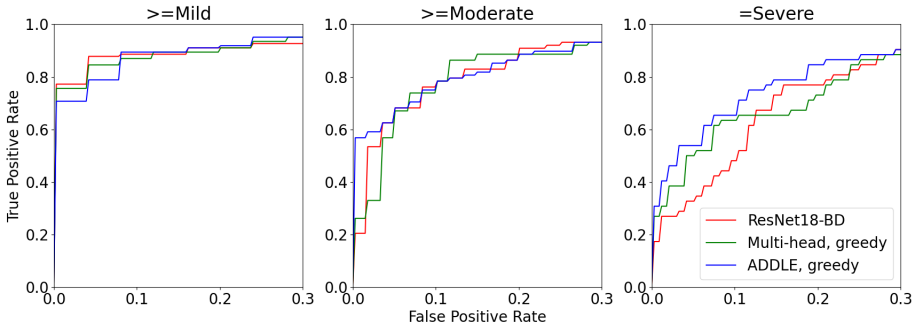


Fig. 2. Partial ROC curves (FPRs ≤ 0.30) on the biopsy-proven test set, excluding JLSL which requires 65 models.

values [13], which is a multi-partite generalization of the AUC [7] that also ranges from 0 to 1, with 1 corresponding to perfect discrimination between the four histopathological grades.

Table 1. Diagnostic performance on the biopsy-proven test set. Note, ResNet18-**HP** is cross-validated on the **HP**-T test set itself, whereas all others are trained on the large-scale **BD** dataset with subjective US labels.

		>= Mild		>= Moderate		= Severe		Params.
Model	JT	AUC_0	AUC_{0P}	AUC_1	AUC_{1P}	AUC_2	AUC_{2P}	(millions)
ResNet-18-**BD**	0.882	0.952	0.876	0.923	0.770	0.869	0.615	11.00
ResNet-18-**HP**	0.816	0.799	0.509	0.872	0.642	0.892	0.676	11.00
JLSL [4] (mean)	0.892	0.956	0.869	0.916	0.736	0.893	0.697	714.95
JLSL [4] (greedy)	0.878	0.944	0.860	0.897	0.722	0.883	0.694	714.95
Multi-head [9] (mean)	0.888	0.956	**0.875**	0.918	0.746	0.879	0.658	11.03
Multi-head [9] (greedy)	0.889	0.955	0.869	0.924	0.764	0.873	0.650	11.03
ADDLE (mean)	0.890	**0.957**	0.873	0.922	0.762	0.886	0.672	11.00
ADDLE (greedy)	**0.898**	0.955	0.864	**0.931**	**0.786**	**0.899**	**0.720**	11.00

Results Table 1 outlines the performance of all tested models on **HP**-T, and Fig. 2 depicts selected partial ROC curves of methods that only require one model. As can be seen, the standard ResNet-18 trained on US labels can post a good JT score and good AUCs. However, it struggles to identify severe steatosis, posting quite poor partial AUCs. As Fig. 2(c) demonstrates, this corresponds to only a sensitivity of 40% at a false positive rate (FPR) of 10%. Overall, ResNet-18-**HP** performs much poorer, even though it was cross-validated on **HP**-T itself and trained with actual histopatholgoical labels. This highlights the importance of training on large-scale data even if rater noise is present. Moving on to the competitor models, they are mostly able to boost the JT

scores. For the most part, any gains are seen in the AUC_2 scores, with JLSL outperforming multi-head. However, for JLSL these gains require training 65 separate models. Moreover, only greedy multi-head is able to match the baseline's AUC_1 scores. Finally, JLSL's greedy rater performance is considerably worse than its mean rater variant, suggesting an overfitting problem that prevents rater performances generalizing from **HP**-V to **HP**-T.

When ADDLE's result are examined, it can be seen that it can boost the AUC_2 by even greater margins, with the greedy rater performing best (partial AUC_2 increases from 0.615 to 0.720). Compared to ResNet-18-**BD**, this is a boost of sensitivity from 40% to 65% at a 10% FPR. Greedy ADDLE can also boost the AUC_1 results (partial AUCs increase from 0.770 to 0.786). Importantly, despite only requiring one model and incurring no practical computational cost over the baseline model, greedy ADDLE can still outperform the much costlier greedy JLSL. When greedy rater selection is not available, ADDLE and JLSL are more comparable, but mean ADDLE achieves this performance at $1/65$ of the training cost.

The ADDLE latent space can itself be analyzed, which is an avenue of analysis not available elsewhere. For instance, as Fig. 3(a) demonstrates, there is considerable difference between the worst and best performing virtual-rater performance. Interpolating between the corresponding latent vectors produces a smooth performance curve. Additionally, as Fig. 3(b) illustrates, when conducting principal components analysis (PCA), varying the first principle component will produce variations in performance, suggesting that the latent embedding is indeed capturing differences in rater abilities. The first 6 principle components explain 75.2% variance, and the last principle component still explains 4.5% variance. These evidences support our choosing of latent embedding dimensionality 10, which is not likely to be further compressed based on the explained variance ratio. The norms of all latent vectors, z, range from 0.40 to 1.86, which is a reasonable range for our choice of $\sigma^2 = 1.0$. However, one interesting fact we observed is that 2-D PCA and 2-D t-SNE plots show no clustering of latent vectors with high performance, which could be a future research direction, and further investigation may provide additional insights into the latent space properties.

4 Conclusion

We introduced ADDLE as an effective approach to deal with subjective ratings using auto-decoded latent variables. ADDLE is highly *expressive*, *i.e.*, modelling rater labels as conditional on the image, *flexible*, *i.e.*, admitting any loss and number of ratings per sample, and *efficient*, *i.e.*, incurring no additional computational cost in training over standard models. We train ADDLE on $36\,602$ subjectively labelled US studies for liver steatosis, by far the largest such dataset used to date. When evaluated on a separate biopsy-proven dataset, ADDLE outperforms standard classifiers as well as leading annotator noise competitors [9,4]. These results indicate that ADDLE can better learn from and exploit subjective labels to produce quantitative steatosis assessments. Given the prevalence of subjective labels in CAD training data, future work should validate ADDLE in other end applications, including for detection and segmentation tasks.

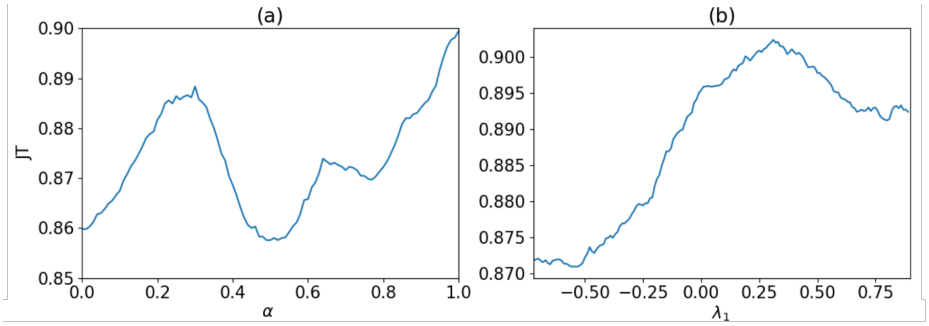


Fig. 3. The latent space and the effects on performance. (a): the test-set JT scores are measured as the latent vector is interploated between the virtual raters with the worst ($\mathbf{z}_0$) and best ($\mathbf{z}_1$) performance, *i.e.*, $\mathbf{z} = \mathbf{z}_0 + \alpha \cdot (\mathbf{z}_1 - \mathbf{z}_0)$. (b): the performance when using the first principle component of the PCA basis, scaled using $\lambda_1 = -0.72, \ldots 0.90$ (range calculated by projecting virtual raters to the first principle component). Graphs of other principle components can be found in the supplementary.

References

1. Biswas, M., Kuppili, V., Edla, D.R., Suri, H.S., Saba, L., Marinhoe, R.T., Sanches, J.M., Suri, J.S.: Symtosis: A liver ultrasound tissue characterization and risk stratification in optimized deep learning paradigm. Computer methods and programs in biomedicine **155**, 165–177 (2018) 3
2. Byra, M., Styczynski, G., Szmigielski, C., Kalinowski, P., Michałowski, Ł., Paluszkiewicz, R., Ziarkiewicz-Wróblewska, B., Zieniewicz, K., Sobieraj, P., Nowicki, A.: Transfer learning with deep convolutional neural network for liver steatosis assessment in ultrasound images. International journal of computer assisted radiology and surgery **13**(12), 1895–1903 (2018) 3
3. Cheng, C.T., Wang, Y., Chen, H.W., Hsiao, P.M., Yeh, C.N., Hsieh, C.H., Miao, S., Xiao, J., Liao, C.H., Lu, L.: A scalable physician-level deep learning algorithm detects universal trauma on pelvic radiographs. Nature communications **12**(1), 1–10 (2021) 1
4. Chou, H., Lee, C.: Every rating matters: Joint learning of subjective labels and individual annotators for speech emotion classification. In: ICASSP 2019 - 2019 IEEE International Conference on Acoustics, Speech and Signal Processing (ICASSP). pp. 5886–5890 (2019) 2, 3, 6, 7, 8
5. Dawid, A.P., Skene, A.M.: Maximum likelihood estimation of observer error-rates using the em algorithm. Journal of the Royal Statistical Society. Series C (Applied Statistics) **28**(1), 20–28 (1979) 2
6. Frank, E., Hall, M.: A Simple Approach to Ordinal Classification. In: De Raedt, L., Flach, P. (eds.) Machine Learning: ECML 2001. pp. 145–156. Lecture Notes in Computer Science, Springer, Berlin, Heidelberg (2001) 6
7. Fürnkranz, J., Hüllermeier, E., Vanderlooy, S.: Binary Decomposition Methods for Multipartite Ranking. In: Buntine, W., Grobelnik, M., Mladenić, D., Shawe-Taylor, J. (eds.) Machine Learning and Knowledge Discovery in Databases. pp. 359–374. Lecture Notes in Computer Science, Springer, Berlin, Heidelberg (2009) 6, 7
8. Greenspan, H., Van Ginneken, B., Summers, R.M.: Guest editorial deep learning in medical imaging: Overview and future promise of an exciting new technique. IEEE Transactions on Medical Imaging **35**(5), 1153–1159 (2016) 1

9. Guan, M., Gulshan, V., Dai, A., Hinton, G.: Who said what: Modeling individual labelers improves classification (2018) 2, 3, 6, 7, 8
10. Gummadi, S., Patel, N., Naringrekar, H., Needleman, L., Lyshchik, A., O'Kane, P., Civan, J., Eisenbrey, J.R.: Automated machine learning in the sonographic diagnosis of non-alcoholic fatty liver disease. ADVANCED ULTRASOUND IN DIAGNOSIS AND THERAPY **4**(3), 176–182 (2020) 3
11. He, K., Zhang, X., Ren, S., Sun, J.: Deep residual learning for image recognition. In: Proceedings of the IEEE conference on computer vision and pattern recognition. pp. 770–778 (2016) 6
12. Hernaez, R., Lazo, M., Bonekamp, S., Kamel, I., Brancati, F.L., Guallar, E., Clark, J.M.: Diagnostic accuracy and reliability of ultrasonography for the detection of fatty liver: A meta-analysis. Hepatology **54**(3), 1082–1090 (2011) 2
13. Jonckheere, A.R.: A distribution-free k-sample test against ordered alternatives. Biometrika **41**(1/2), 133–145 (1954) 7
14. Khetan, A., Lipton, Z.C., Anandkumar, A.: Learning from noisy singly-labeled data. In: International Conference on Learning Representations (2018) 2
15. Li, B., Yan, K., Tai, D.I., Huo, Y., Lu, L., Xiao, J., Harrison, A.P.: Reliable liver fibrosis assessment from ultrasound using global hetero-image fusion and view-specific parameterization. In: International Conference on Medical Image Computing and Computer-Assisted Intervention. pp. 606–615. Springer (2020) 3, 6
16. Park, J.J., Florence, P., Straub, J., Newcombe, R., Lovegrove, S.: Deepsdf: Learning continuous signed distance functions for shape representation. In: Proceedings of the IEEE Conference on Computer Vision and Pattern Recognition. pp. 165–174 (2019) 3
17. Reddy, D.S., Bharath, R., Rajalakshmi, P.: A novel computer-aided diagnosis framework using deep learning for classification of fatty liver disease in ultrasound imaging. In: 2018 IEEE 20th International Conference on e-Health Networking, Applications and Services (Healthcom). pp. 1–5. IEEE (2018) 3
18. Suzuki, K.: Overview of deep learning in medical imaging. Radiological physics and technology **10**(3), 257–273 (2017) 1
19. Tanno, R., Saeedi, A., Sankaranarayanan, S., Alexander, D.C., Silberman, N.: Learning from noisy labels by regularized estimation of annotator confusion. In: 2019 IEEE/CVF Conference on Computer Vision and Pattern Recognition (CVPR). pp. 11236–11245 (2019) 2
20. Warfield, S.K., Zou, K.H., Wells, W.M.: Simultaneous truth and performance level estimation (staple): an algorithm for the validation of image segmentation. IEEE Transactions on Medical Imaging **23**(7), 903–921 (2004) 2
21. Welinder, P., Branson, S., Perona, P., Belongie, S.: The multidimensional wisdom of crowds. In: Lafferty, J., Williams, C., Shawe-Taylor, J., Zemel, R., Culotta, A. (eds.) Advances in Neural Information Processing Systems. vol. 23. Curran Associates, Inc. (2010) 2
22. Willemink, M.J., Koszek, W.A., Hardell, C., Wu, J., Fleischmann, D., Harvey, H., Folio, L.R., Summers, R.M., Rubin, D.L., Lungren, M.P.: Preparing medical imaging data for machine learning. Radiology **295**(1), 4–15 (2020) 1
23. Wu, K., Chen, X., Ding, M.: Deep learning based classification of focal liver lesions with contrast-enhanced ultrasound. Optik **125**(15), 4057–4063 (2014) 3
24. Younossi, Z., Anstee, Q.M., Marietti, M., Hardy, T., Henry, L., Eslam, M., George, J., Bugianesi, E.: Global burden of NAFLD and NASH: trends, predictions, risk factors and prevention. Nature Reviews Gastroenterology & Hepatology **15**(1), 11–20 (Jan 2018), number: 1 Publisher: Nature Publishing Group 2
25. Yu, S., Zhou, H.Y., Ma, K., Bian, C., Chu, C., Liu, H., Zheng, Y.: Difficulty-aware glaucoma classification with multi-rater consensus modeling. In: International Conference on Medical Image Computing and Computer-Assisted Intervention. pp. 741–750. Springer (2020) 2